

Article

# Automatic Determination of the Parameters of Electrical Signals and Functional Responses of Plants Using the Wavelet Transformation Method

Maxim Mudrilov, Lyubov Katicheva, Maria Ladeynova, Irina Balalaeva , Vladimir Sukhov   
and Vladimir Vodeneev \* 

Department of Biophysics, National Research Lobachevsky State University of Nizhny Novgorod, 23 Gagarin Avenue, Nizhny Novgorod 603950, Russia; mtengri@yandex.ru (M.M.); katicheva\_la@mail.ru (L.K.); ladeynova.m@yandex.ru (M.L.); irin-b@mail.ru (I.B.); vssuh@mail.ru (V.S.)

\* Correspondence: v.vodeneev@mail.ru

Received: 15 October 2019; Accepted: 25 December 2019; Published: 28 December 2019



**Abstract:** Smart agriculture management systems with real-time control of plant health and vegetation are recognized as one of the crucial technologies determining agriculture development, playing a fundamental role in reducing yield losses and improving product quality. The earliest plant responses to various adverse factors are propagating stress signals, including electrical ones, and the changes in physiological processes induced by them. Among the latter, photosynthesis is of particular interest due to its key role in the production process. Of practical importance, photosynthesis activity can be registered not only in contact mode but by remote sensing using optical methods. The aim of the present work was to develop the approach to automatic determination of the main parameters of electrical signals and changes in photosynthesis activity and transpiration using continuous wavelet transform (CWT). Applying CWT based on derivatives of the Gaussian function allows accurate determination of the parameters of electrical signals as well as induced physiological responses. Moreover, CWT was applied for spatio-temporal mapping of the photosynthesis response to stress factors in pea leaf. The offered approach allowed automatic identification of the response start time in every pixel and visualization of the change propagation front. The results indicate high potential of CWT for automatic assessment of plants stress, including monitoring of plant health in large-scale agricultural lands and automated fields.

**Keywords:** electrical signal; photosynthesis; smart agriculture; stress in plant; wavelet transform

## 1. Introduction

The productivity of agricultural plants is known to be directly dependent on environmental conditions. High adaptability of plants to abiotic and biotic factors leads to minimization of crop losses. Adaptation is based on a coordinated change in the activity of a number of physiological processes controlled by the signaling system [1–4]. The crucial role in plant adaptation to rapidly changing environmental factors such as temperature, illumination, etc., is played by distant signals and functional changes caused by them [4–7]. The existence of several types of signals in plants is assumed: chemical, hydraulic, and electrical [6]. The fastest propagating signals of plants are ones of a physical nature, such as electrical signals whose speed of propagation can reach more than 10 cm/s, whereas for chemical signals it is less than 0.2 cm/s. Besides the action potential which is universal for all living organisms, the plant-specific variation potential (VP) and system potential [6,8,9] can be distinguished.

VP plays a particular role due to its generation in response to wide range of damaging stimuli, including mechanical wounding, herbivore attack, heating, etc. This type of electrical signal is a wave

of membrane depolarization with an amplitude of several tens of mV, characterized by an irregular and prolonged phase of repolarization, and is not subjected to the all-or-nothing rule: the parameters of the VP are dependent on the type and intensity of the stimulus [3,6,8]. For example, the probability of VP occurrence and its amplitude rises with increasing area of the tomato leaf subjected to mechanical damage [10]. Burn is a strong stimulus known to inevitably cause the propagation of high-amplitude VP, and therefore this stimulus is commonly used as a standard VP inducer in laboratory conditions. A more physiological stimulus, namely, gradual local heating, also induces VP, which propagates over a long distance with greater amplitude compared to mechanical damage [11]. During VP propagation, a signal decrement is observed—the amplitude and VP propagation velocity decrease with increasing distance from the wounding area [3,6,8,12,13].

VP generation is associated with ion flows through the membrane of plant cells. The first step in VP generation is an activation of calcium channels with the subsequent entry of  $\text{Ca}^{2+}$  into the cell. Activation of calcium channels may be caused by a hydraulic or chemical signal propagating from the local wounding area [3,5,6,8,14]. The entry of  $\text{Ca}^{2+}$  into cell results in  $\text{H}^+$ -ATPase inactivation and anion channel activation, both leading to depolarization. The repolarization phase is associated with the restoration of  $\text{H}^+$ -ATPase activity due to the return of the  $\text{Ca}^{2+}$  concentration to initial levels [3,5,6,8].

Of particular importance is the VP role in modifying the activity of a number of physiological processes, including photosynthesis, respiration, relative concentrations of plant hormones, gene expression profile, etc. [3,5–7,15]. The possible regulation of photosynthesis activity by electrical signals has attracted the most attention of the research community due to the key role of photosynthesis in the production process. The VP-induced photosynthetic response is a transient decrease in activity, which starts virtually without a lag period. The reason for the photosynthesis inactivation is a shift in the cytosolic calcium concentration and cytosolic and apoplastic pH, which arises due to VP generation [7,12,16–19]. The parameters of photosynthesis activity are highly informative indicators of plant response to stress. In addition, it is necessary to note the high development of technology that provides high accuracy and simplicity of measurements of photosynthesis activity in laboratory and field conditions.

Taking into account the fact that VP is a typical electrical signal induced by adverse factors, the recording of such signals and/or the induced changes in photosynthetic activity can be used to rapidly assess the functional state of agricultural plants. Rapid assessment of the state of plants is necessary for the timely adoption of measures aimed at reducing the negative impact of the stress factor. However, the problem of collating the dynamics of the electrical signal with the functional response has still not been completely solved. A diagnostic system recording and analyzing the electrical signals and/or the photosynthesis responses can become a basic element for an automated decision-making system that provides feedback.

A substantial consequence of distant signal propagation and induced functional changes is an increase in plant resistance to adverse factors [20–25]. The establishment of the correlation between the parameters of stress and induced changes of photosynthesis activity with the development of plant resistance to stress factors [26], in particular the resistance of the photosynthetic apparatus to heating [21,23,24], allows the creation of approaches and methods for selecting the most promising genetic lines in the early stages of plant breeding.

The application of these approaches in agriculture research requires the processing of large amounts of data, which can only be effective in an automatic mode. The same task is important for research on spatio-temporal mapping of signals using multi-electrode array [27] and for photosynthesis studies [11,17]. An accurate automatic detection of signal parameters, including the reaction start time, amplitude, and propagation speed is of great importance. Manual processing not only is extremely time-consuming, but can produce errors due to the subjectivity in assessment of vague and dim signal records as well as signals of a complex irregular shape. Nonetheless, there are no common algorithms for automatic determination of the electrical signals parameters and plant functional responses induced by them.

Wavelet transform (WT) is a promising tool to meet the challenge of an accurate automatic determining of signal and reaction parameters. The main difference between WT and another popular method of spectral analysis—Fourier transform—is WT's ability to obtain not only the frequency but also the time characteristic of the analyzed signal [28,29]. This feature of WT, as well as the availability of a wide range of the mother wavelets (basis functions used for the transformation), promoted WT's wide applications for processing and analysis of biological signals, in particular for processing of neural impulses [30–33], analysis of population shifts in environmental studies [34], biomolecule studies [35,36], assessment of changes in chlorophyll content [37], water balance [38], pathogen identification [39], etc. WT was also applied to monitor the status of agricultural crops, including the processing of large amount of data on year/season dynamics, and analysis of images obtained by remote sensing [40–42]. There are two main types of wavelet transform—continuous (CWT) and discrete wavelet transform (DWT). In our work, CWT was used due to the greater simplicity of its application and interpretation of the results, as well as its good ability to identify signal features [28,41].

The aim of the present work was to apply WT for analysis of electrical signals and changes of photosynthesis activity induced by them in higher plants. We demonstrated an applicability of WT for an accurate automatic determining of amplitude and start time of both electrical signal and photosynthetic response as well as for spatio-temporal mapping of the photosynthetic activity.

## 2. Materials and Methods

### 2.1. Experimental Methods

#### 2.1.1. Plant Material and Stimulation

Studies were carried out on 14–21-day-old seedlings of wheat (*Triticum aestivum* L.) and pea (*Pisum sativum* L.) cultivated hydroponically in a Binder KBW 240 (Germany) plant growth chamber at 24 °C under a 16/8-h (light/dark) photoperiod.

Electrical signals and photosynthetic reactions were induced by two types of stimuli [11]. The first type of stimulation was a gradual heating simulating heat shock in natural conditions. The leaf was placed in a cuvette filled with water and gradually heated until the VP generation was registered. In all the experiments the VP generation was observed at temperatures not exceeding 55 °C. The second type of stimulation was a commonly used experimental approach for VP induction, specifically, a burn of a leaf tip with an open flame.

#### 2.1.2. Intracellular Measurement of Electrical Activity

The absolute value of the membrane potential was recorded using an electrophysiological device for microelectrode biopotential registration based on the SliceScope Pro microscope (Scientifica, Uckfield, UK), amplifier Multiclamp 700 B (Molecular Devices, Sunnyvale, CA, USA), and a low-noise data acquisition system for electrophysiology DIGIDATA 1550 (Molecular Devices, Sunnyvale, CA, USA). Measurements were performed at 10 Hz. The seedling was placed at the side of the microscope, and the leaf was fixed horizontally. Part of the leaf was placed in a cuvette filled with artificial pond water (APW), which comprised 0.1 mMNaCl, 1 mMKCl, and 0.5 mM $\text{CaCl}_2$ . Single-barreled microelectrodes were fabricated from 1.2-mm (outer diameter) borosilicate glass tubing. Capillaries with a tip diameter of about 0.5  $\mu\text{m}$  were pulled in a horizontal pipette puller P-97 (Sutter Instrument, Novato, CA, USA) and filled with 100 mM KCl. The measuring electrode was inserted into the parenchymal cell of the second to third layer of the leaf lamina by motorized manipulators under visual control using the microscope objective lens. The reference electrode was immersed into a cuvette with APW. The distance between the stimulation and registration zones was equal to 5 cm.

### 2.1.3. Extracellular Measurement of Electrical Activity

To estimate the parameters of the generation and propagation of electrical signals through the whole plant, the electrical signals were recorded (at 1 Hz) extracellularly using Ag<sup>+</sup>/AgCl electrodes (Gomel Plant of Measuring Devices, Gomel, Belarus). The electrodes were connected to a high-impedance amplifier IPL-113 (Semico, Novosibirsk, Russia) and a personal computer (PC). The measuring electrodes were set in contact to the pea stem or the second wheat leaf at five different points. The distances between the stimulation zone and the electrodes positions are indicated in the figures. The reference electrode was placed in APW solution bathing the roots of the seedling. The reaction start time and amplitude at different sites of the plant were analyzed.

### 2.1.4. Measurement of Photosynthetic Parameters and Transpiration

Registration of photosynthesis activity and transpiration was carried out using a system allowing simultaneous recording of gas exchange parameters (infrared gas analyzer GFS-3000, Heinz Walz GmbH, Effeltrich, Germany) and parameters of photosystems I and II (PAM-fluorimeter (Pulse Amplitude Modulation fluorimeter) Dual-PAM-100 Heinz Walz GmbH, Effeltrich, Germany). The measurements were carried out under controlled conditions: an intensity of actinic blue light of 239  $\mu\text{mol m}^{-2} \text{s}^{-1}$ , external CO<sub>2</sub> concentration of 360  $\mu\text{L L}^{-1}$ , and relative air humidity and temperature of about 70% and 23 °C, respectively. The assimilation rate (A) and transpiration intensity (E) were registered with frequency of once per second after 15 min dark adaptation and calculated according to Von Caemmerer and Farquhar [43]. The dark fluorescence yield (F<sub>0</sub>) and the maximal fluorescence yield (F<sub>m</sub>) of photosystem II (PSII) were measured after dark adaptation for 15 min. The maximal change of the P700 signal (P<sub>m</sub>) reflecting the maximal P700 oxidation in photosystem I (PSI) was measured after preliminary illumination by far red light for 20 s. After that the actinic light was switched on; under light conditions, steady-state fluorescence yield (F), maximal fluorescence yield (F<sub>m</sub>'), steady-state P700 signal (P), and maximal change of the P700 signal (P<sub>m</sub>') were measured with saturating pulses given every 20 s. Quantum yields of PSI (Y(I)) and PSII (Y(II)) were calculated according to Klughammer and Schreiber [44] and Maxwell and Johnson [45], respectively. Non-photochemical quenching of fluorescence in PSII (NPQ) was calculated according to Maxwell and Johnson (2000). Measurements were performed on intact plants acclimated to a measuring system for 1.5 h or more.

The spatio-temporal distribution of photosynthetic activity in a leaf lamina was investigated by PAM-imaging (Imaging-PAM M-Series MINI-version, Heinz Walz GmbH, Effeltrich, Germany). The measurements were carried out after plant acclimation to a measuring system for 1.5 h and 15 min dark adaptation at intensity of actinic blue light of 239  $\mu\text{mol m}^{-2} \text{s}^{-1}$  and saturating pulses given every 10 s. Y (PSII) and NPQ were calculated for every saturation pulse.

Each series of experiments comprised 4–8 repetitions; every replicate was performed on a separate plant.

## 2.2. Wavelet Transform

The general equation for continuous wavelet transform (CWT) is:

$$W = \int_{-\infty}^{\infty} x(t)\psi(t)dt$$

where  $W$  is wavelet coefficient,  $x(t)$  is the analyzed record, and  $\psi(t)$  is a basis function, the mother wavelet, that can be shifted (translated) and scaled (stretched or compressed) to produce a series of continuous wavelets [33,46,47]:

$$\psi(t) = \frac{1}{\sqrt{\alpha}}\psi\left(\frac{t-\tau}{\alpha}\right)$$

where  $\alpha$  and  $\tau$  are positive numbers representing the scaling and shifting factors, respectively.

The wavelet coefficient  $W$  will have maxima where the input signal most closely resembles the analysis template, i.e., the mother wavelet. In this study, used transforms based on first to third orders derivatives of the Gaussian function were selected as the mother wavelet due to their similarity to the analyzed records. The CWT of the input experimental record resulted in scalogram: visual displaying of wavelet transform with axes representing shift, scale and  $W$  value shown in pseudocolors.

The scheme of automatic processing of the analyzed records (raw records of electrical and photosynthetic activity) is presented in Figure 1.

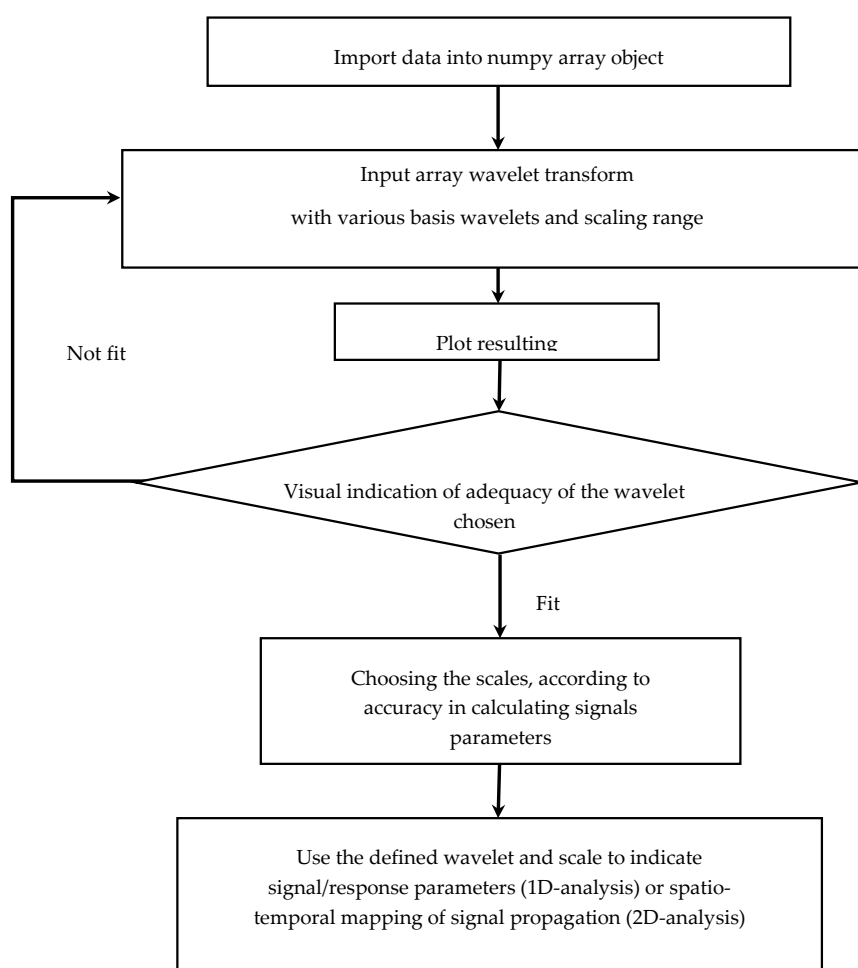


**Figure 1.** The algorithm of the continuous wavelet transform of the input record. The input data were the records of electric potentials and parameters of photosynthetic activity: quantum yields of photosystems I and II, and non-photochemical quenching. The effectiveness of machine processing was verified using the Bland–Altman method.

For 2D analysis, we obtained a 3D matrix containing in each 2D slice the distribution pattern of the signal intensity of the photosynthetic response, and the number of such slices (z-axis) was responsible for the time of registration. Calculations to determine the start time of the reaction for each pixel were performed using the same wavelet analysis as in the one-dimensional analysis. For presentation of the CWT result, the final matrix was recalculated into the simplest binary form, where the value “1” was assigned to a particular pixel  $X, Y, Z$  if it corresponded to the start of the reaction.

The Bland–Altman method was used to evaluate the accuracy of the automatic processing. The principle of the method is based on determining the range, within which 95% of the differences between the two techniques, in this case between manual and automatic processing, are included. In addition, the mean deviation between the two techniques was calculated. The reaction start time at

manual processing was determined as the beginning of the rapid depolarization in the signal recording, namely. The amplitude of the reaction was determined as the difference between the values at the reaction start time and its peak value [48,49].

### 3. Results

#### 3.1. Electrical Signals Analysis

The selection of the optimal mother wavelet function for the analysis of the electrical signal induced by the plant damage—variation potential—was the first objective of the study. Variation potential induced by burn of the wheat leaf tip was registered by microelectrode technique distantly from the local damage area (Figure 2). The electrical signal represents a transient depolarization with an amplitude of about 60 mV, with a fast depolarization phase (not exceeding 10 s) and a long (hundred seconds) repolarization phase, which are typical parameters for VP [6,8]. Since a typical signal is a transient membrane potential increase, a soliton-like Gaussian function was applied as a basis for continuous wavelet transform [29]. The transforms based on first to third orders derivatives of the Gaussian function were compared. CWT results are presented in Figure 2 as a scalogram with color-coded relative magnitude ( $W$ ) at different shifting factors ( $\tau$ ) and scales ( $\alpha$ ). The criterion for the selection of the mother wavelet was the presence of a single, most pronounced extremum (on scalograms indicated in red), localized in at the start of the reaction. The CWT extremes were most clearly expressed in the case of the second-order Gaussian derivative (Gaus-2), that is apparently due to the two-phase form of both the electrical signal and the basis wavelet (Figure 2C). This type of the mother wavelet was further applied for the analysis of the electrical signals registered extracellularly.

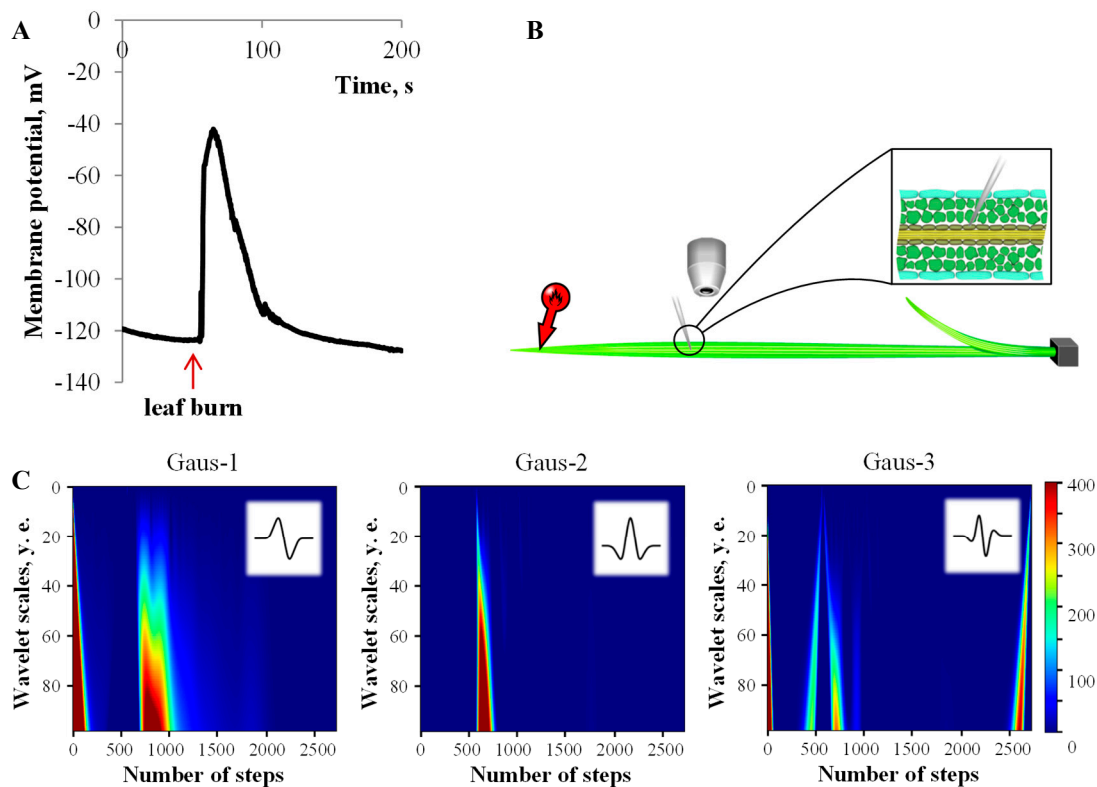


**Figure 2.** The typical intracellular record of the variation potential induced by burn of the wheat leaf tip and registered from the wheat cell by the microelectrode technique (A), a scheme of the experiment (B), and scalograms of the signal record wavelet transform by means of first- to third-order Gaussian bases (C). One step equals 0.1 s. The reaction started at 56 s, expressed as a local maximum on a scalogram.

Extracellular registration of electrical activity is the only option for multichannel recording in plants, allowing for the estimation of the propagation parameters of electrical signals in plants. It is also the most suitable approach for simultaneous registration of electrical activity and parameters of plant functional activity [18,22,50–52]. The typical multichannel records of heat-induced electrical signals in wheat and pea are presented in Figure 3A,B, respectively. Extracellularly registered signals have a reversed polarity. The essential difference of the extracellular recordings from the intracellular is their “blurriness”: a less pronounced peak of depolarization, a lack of a clear starting point for depolarization. The “blur” is resulted from the superposition of electrical signals from many cells when macroelectrodes are used. The most blurred are the signals recorded at long distance from the local damage area that is caused by VP decrement as it propagates [8]. These features make it difficult to determine the reaction start time.

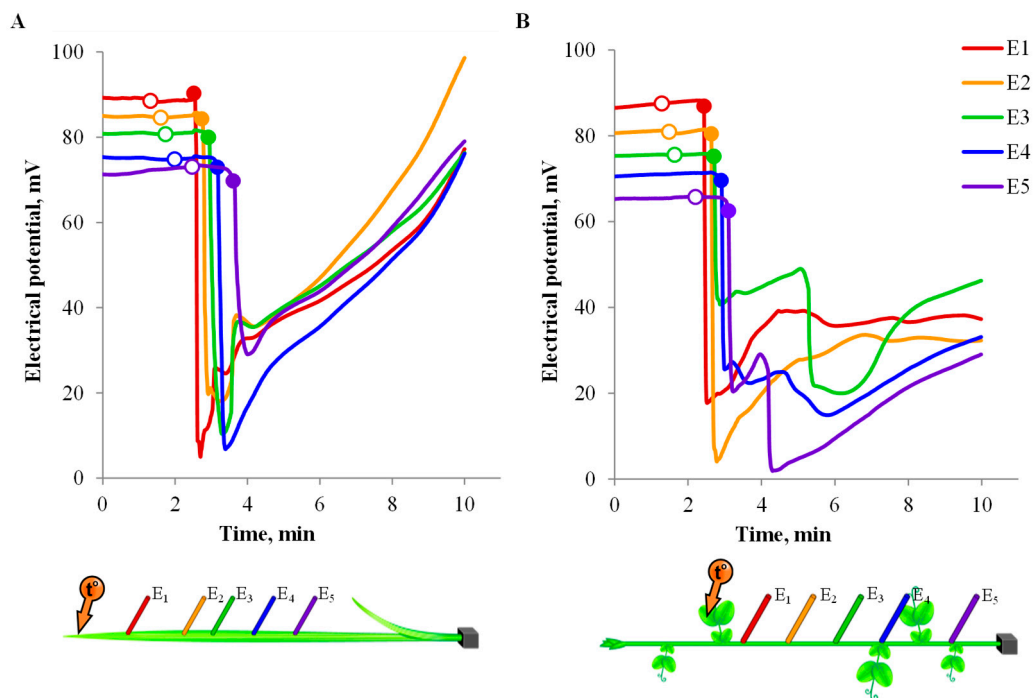


**Figure 3.** The typical extracellular multichannel record of variation potential induced by heating of the wheat leaf tip (A), or heating of the top leaf of the pea seedling (B). The circles show the start time of the reaction, calculated by machine processing. Open circles, reaction start at high scales (100); filled circles, at optimal scales (10 and 5 for wheat and pea, respectively). The scheme of induction and recording of variation potential is shown below. The distances between the stimulated area in wheat and the electrodes E1, E2, E3, E4, E5 were 1.5, 3, 4.5, 6, and 7.5 cm, respectively. The distances between the stimulated area in pea and the electrodes E1, E2, E3, E4, E5 were 3, 4.5, 6, 7.5, and 10.5 cm, respectively.

Taking into account that the signal shape for intra- and extracellular recording is similar for analysis (except a reversed polarity and somewhat longer repolarization), after verification (data not shown) the same type of the mother wavelet, Gauss-2, was used. The determination of the W dependence on scale values was performed (Supplementary Tables S1 and S2). However, the reaction start time determined at high scales (Figure 3, open circles) poorly corresponds to the real start of the depolarization. As a result, the VP parameters (amplitude, duration, velocity) are calculated with an error. To meet the problem, the choice of an optimal scale factors value was based on analysis of the agreement between the amplitudes and the reaction start times determined by manual and automatic processing. The highest agreement for pea was found to be at scale value equal to 5 (Figure 3B, filled circles; Figure 4A); for wheat, to 10 (Figure 3A, filled circles). This was the case for signals registered with all electrodes (E1–E5)

arranged at various distances from the stimulation site. The values of amplitudes and reaction start time obtained using manual and automatic processing are shown in Supplementary Tables S3–S6, respectively.

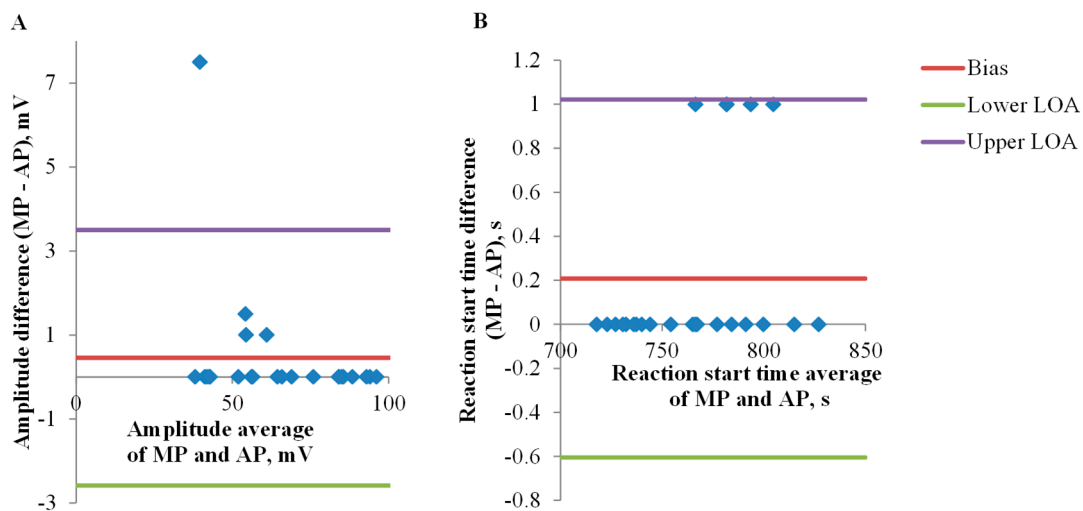


**Figure 4.** Bland–Altman plot of differences between values of variation potential amplitude (A) and reaction start time (B) in pea seedlings determined by manual (MP) and automatic (AP) processing. Gauss-2 basis function and scale 5 were used for continuous wavelet transform (CWT). The averaged values of the MP and AP determined parameters are plotted on the X-axis; the differences between the values obtained by MP and AP are plotted on the Y-axis. Bias is the average of the deviations between manual and machine processing. LOAs are limits of agreement, within which 95% of the differences between MP and AP measurement are included.

### 3.2. One-Dimensional Analysis of Photosynthetic Activity

The electrical signal propagation in plants causes a change in the activity of a number of physiological processes, among which researchers focus on photosynthesis [12,17,18,53,54]. We have studied a number of parameters of the photosynthetic response, including quantum yields of photosystems I and II (Y (I) and Y (II)), non-photochemical fluorescence quenching (NPQ), rate of CO<sub>2</sub> assimilation (A), and level of transpiration (E). The typical records of the photosynthesis parameters changes induced by variation potential are shown in Figure 5A,B. VP propagation lead to a decrease in photosynthesis activity, which is manifested in reduced assimilation and transpiration, lower quantum yields of photosystems I and II, and increased non-photochemical quenching. This rapid decrease in the activity of photosynthesis is followed by a recovery which is very slow compared to the duration of the electrical signal. It should be noted that the determined parameters of the photosynthesis response in pea seedlings induced by variation potential are in good agreement with the data obtained by other research groups with various plant objects, including mimosa [17], poplar [18], corn [19], etc. In the mentioned works, the temporal dynamics of the photosynthetic response was similar to each other and to the one registered in our experiments: the rate of CO<sub>2</sub> assimilation decreased by 30–100%, and Y (II) decreased from 0.6 to 0.2. The choice of wavelet type for transformation was based on Y (II) dynamics, due to the importance of this parameter for evaluation the activity of the photosynthesis apparatus and the possibility of its measuring without dark adaptation in field conditions. As in the previous case with the electrical signal, the first- to third-order derivatives of the Gaussian function were considered (Figure 5C). The CWT extremes were most pronounced after transformation of YII dynamics with Gauss-1, which corresponds to a one-phase change of the parameters of photosynthetic activity. Such an analysis was also performed for the other types of the functional response, demonstrating optimal use of Gauss-1 compared to Gauss-2 and Gauss-3 (data not shown). The range of optimal scale values was established using Bland–Altman analysis for every type of the functional response.

Wavelet transform allows to determine the reaction start time and, as a result, to calculate the parameters of the photosynthetic response (Figure 5), which are coincided with manually determined (Supplementary Table S7). This makes possible the simultaneous assessment of the electrical signal and the functional response dynamics for the subsequent study of their relationship. The obtained results demonstrate an applicability of Gauss wavelets for analysis of changes in various parameters in plants.

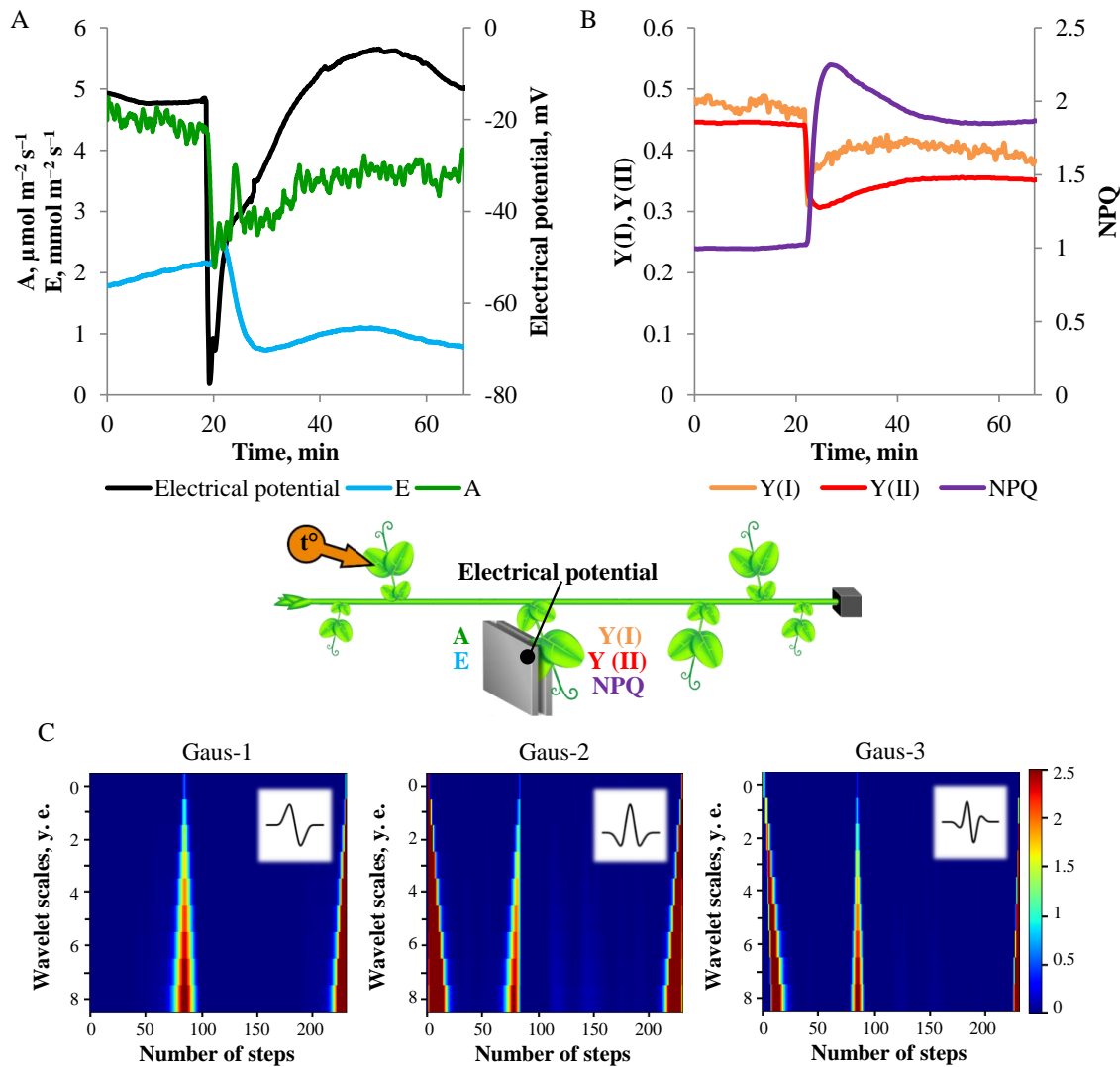


**Figure 5.** The typical record of VP-induced changes in (A) rate of CO<sub>2</sub> assimilation ( $A$ ,  $\mu\text{mol s}^{-1} \text{m}^{-2}$ ) and level of transpiration ( $E$ ,  $\text{mmol s}^{-1} \text{m}^{-2}$ ); (B) parameters of photosynthesis (NPQ,  $Y(I)$ ,  $Y(II)$ ). The decrease in  $Y(I)$ ,  $Y(II)$ ,  $A$  and the increase in NPQ indicate a suppression of photosynthesis. The scheme of the experiment is shown: VP was induced by heating of the top leaf of pea seedling; the measurements were performed on an un-wounded leaf. (C) Scalograms of  $Y(II)$  dynamics wavelet transformation by means of first- to third-order Gaussian bases. One step is equal to 20 s. The reaction started at 23 min, that is expressed as a local maximum on a scalogram. NPQ: non-photochemical quenching; VP: variation potential.

### 3.3. Spatio-Temporal Mapping of the Photosynthetic Activity

The 2D imaging methods for recording the space-time distribution of photosynthesis activity have become widespread along with one-dimensional records of the photosynthesis activity [17,18]. In Figure 6, the dynamics of  $Y(II)$  changes induced by VP propagation to an untreated leaf are presented. VP caused the gradual propagation of the  $Y(II)$  decrease over the area of the leaf lamina; however,

visual determination of the front of the photosynthesis response is complicated due to the unclear border of the reaction. Thereby, the proposed for 1D-records method for determining the signal start time based on wavelet transform was applied to the 2D image of the photosynthesis activity. The Y (II) was chosen to monitor the whole leaf response due to the above mentioned features of this parameter. The same wavelet base (Gauss-1) and scale parameters were applied as in the previous section. As a result of the convolution, a 3D matrix of values was obtained, the z-axis of which corresponded to the time. The binary representation was used with changing pixel color from black to white if the Y (II) reaction had started. Such a representation allowed us to clearly visualize the features of the front propagation of the photosynthesis response. In the given example, one can see a faster propagation of the reaction along the edges of the leaf lamina and a slower one in the center. The propagation velocity for Y (II) changes was assumed to be 0.5–0.8 mm/s.

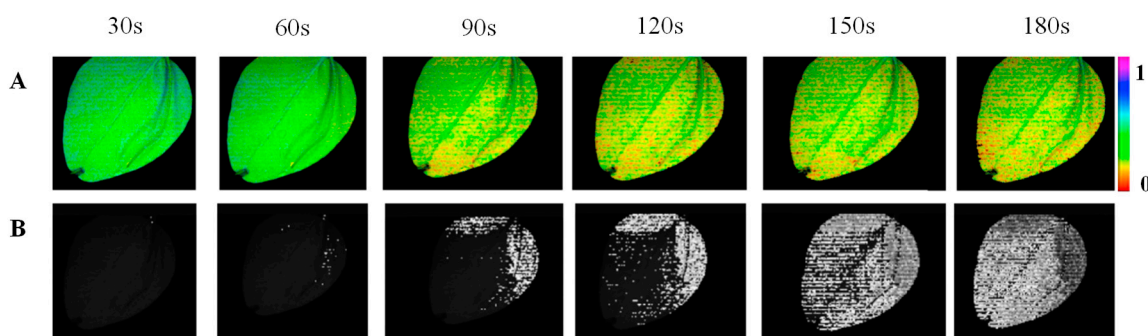


**Figure 6.** The typical images representing the burn-induced spatio-temporal dynamics of Y (II) in pea leaf: the pseudocolor-coded PAM-images of the same untreated leaf at various time points after the stimulation (A), and a binary representation of the CWT results of the initial images (B). The pixel becomes white if the reaction reaches the point. The time after the stimulation (burn of the first leaf) is indicated.

#### 4. Discussion

Wavelet analysis is widely used in biology in such diverse areas as the analysis of brain activity [30], heart rate [55,56], patterns in bird songs [57], environmental studies [34,58,59], and so on. A typical problem of biological signals that is successfully solved using wavelet transform and spectral analysis is a low signal-to-noise ratio [31,32,40].

For the electrical signals analyzed in the present work and the photosynthesis responses they cause, the signal amplitude significantly exceeds the average noise level. At the same time, an objective assessment of the parameters of the signals, including the reaction start time, is a rather complicated task. It was reported by Astafyeva [28] that simple signals such as monotonous decay or biphasic dynamics of the analyzed parameter (that is the case for electrical and photosynthesis activity registered in the present work) can be analyzed using CWT with simple wavelets such as Gaussian function and its first- and second-order derivatives. The selection of the optimal wavelet type and its scale, as we have demonstrated, provides the possibility to correctly determine the parameters of electrical and photosynthetic reactions (Figures 3–5). For instance, the biphasic changes in the electric potential that occur during the variation potential generation correspond quite well to a wavelet of the Gauss-2 type.

Another type of wavelet applied in the work is Gauss-1, which is well suited for analyzing single-phase dynamics (or dynamics with a significantly longer recovery time compared to the initial changes) that occur in the case of stress-induced changes in photosynthesis activity. In this case, the choice of optimal scale values also allowed the accurate and reliable automatic determination of the parameters of photosynthesis response, such as start time and amplitudes for induced changes of Y (I), Y (II), NPQ, and assimilation of CO<sub>2</sub>, as well as intensity of transpiration. A good agreement between the results of automatic and manual processing allows us to talk about the possibility of successful application of WT in practice.

Simultaneous objective assessment of the reaction start time for a large set of parameters potentially makes it possible to assume and verify the causal relationships of the analyzed processes. Thus, it was revealed that the start of changes in transpiration level is in some cases ahead of the electrical signal, which indicates the presence of a factor of a different nature that induces the response of transpiration [50]. At the same time, the sequence “the electrical signal—the change in photosynthesis activity” observed in all the experiments is in line with the point of view that the shift in ionic concentrations induced by the electrical signal is in turn an inducer of the photosynthetic response [3,7,12,19,52,60–62].

In addition to the demonstrated ability to estimate the parameters of a specific reaction, wavelet transform is successfully used to extract the signals from noise and subsequently classify them by type [63–65]. In particular, the use of WT makes it possible to detect changes in biological systems at earlier stages in comparison with manual analysis. Thus, the plant stress-reaction to cooling and shading (detected by the chlorophyll fluorescence) was revealed after 1 h of exposure using wavelet transform and only after 24 h without processing [66].

It is necessary to note the applications of other approaches for automatic signal processing in plants, including use of different types of classifiers [63], interval arithmetic [67], Fourier transform [64], vector computing [65,67], and multiple neural network learning algorithms [67,68]. The methods based on combination of several approaches, including those using WT, seem to be the most effective [63]. Using the method of a polynomial curve fitting in combination with a quadratic discriminant analysis helped to distinguish the response of plants to ozone, sodium chloride and sulfuric acid with approximately 90% accuracy [69]. An even higher efficiency was shown by the method of recognition of an action potential based on a dynamic difference threshold with subsequent incremental pattern matching [68].

In general, we can conclude that the approach proposed in this work has its own niche to be applied. The most obvious areas of its use are the automation of determining the signal characteristics in plants during large-scale laboratory and possibly, field studies, as well as the mapping of the spatio-temporal dynamics of certain parameters. The latter was shown by the example of analyzing changes in the photosynthesis activity within an area of a single leaf of a pea seedling (Figure 6).

The CWT analysis allowed us to produce an easily perceived and interpretable map of the spatial and temporal activity of photosynthesis, and to clearly define the boundaries of the leaf areas with the initial and modified photosynthesis activity that cannot be performed when analyzing the original image (compare Figure 6A,B). The proposed approach can be applied not only for analysis of changes in a single leaf in the laboratory conditions, as shown in this work, but also for processing of large-scale images, such as maps of agricultural land obtained using unmanned aerial vehicles and satellites, and those representing various indices of plants health and vegetation, such as normalized difference vegetation index (NDVI), photochemical reflectance index (PRI), etc. In particular, the changes in photosynthesis, induced by direct action of stressors [70–72] or by propagation of electrical signals [73], can induce changes in PRI, which is widely used in remote sensing of the plant physiological states [74–76]. Analysis of the propagation front of the changes of particular parameters will allow for the discrimination of the factors that induce the detected changes: infection with certain pathogens, water scarcity, mineral deficiency, etc.

## 5. Conclusions

In the present work, we applied the CWT method to determine the parameters of the distant electrical signals in plants and the physiological responses induced by stress, as well as to map the spatio-temporal dynamics of photosynthesis activity. The selection of the optimal mother wavelet function and optimal scale factors value allowed us to obtain a good agreement between the parameters determined by the proposed method and the manual processing. The CWT method significantly expands the possibilities of analyzing the spatial dynamics of certain parameters. It was successfully applied for studying the burn-induced spatio-temporal dynamics of photosynthetic activity in a plant leaf. The proposed approach can be used for the automation of screening studies of plant resistance in

controlled conditions, in particular when phenotyping, and possibly for assessing the physiological state of plants in large-scale agricultural land and environmental observations.

**Supplementary Materials:** The following are available online at <http://www.mdpi.com/2077-0472/10/1/7/s1>, Table S1. Average maximum wavelet coefficients (Wmax) obtained at continuous wavelet transform (CWT) procedure with different scales for five records of multielectrode electrical potential registration in pea seedlings, Table S2. Average maximum wavelet coefficients (Wmax) obtained at continuous wavelet transform (CWT) procedure with different scales for five records of multielectrode electrical potential registration in wheat seedlings, Table S3. Amplitude (mV) of the heating-induced variation potential (VP) in pea seedlings, calculated using manual (MP) or automatic processing (AP) (scale 5), Table S4. Amplitude (mV) of the heating-induced variation potential (VP) in wheat seedlings, calculated using manual (MP) or automatic processing (AP) (scale 10), Table S5. The start time (s) of the heating-induced variation potential (VP) in pea seedlings, calculated using manual (MP) or automatic processing (AP) (scale 5), Table S6. The start time (s) of the heating-induced variation potential (VP) in wheat seedling, calculated using manual (MP) or automatic processing (AP) (scale 10), Table S7. Amplitudes of VP-induced changes in CO<sub>2</sub> assimilation rate (A,  $\mu\text{mol m}^{-2}\cdot\text{s}^{-1}$ ), transpiration level (E,  $\text{mmol m}^{-2}\cdot\text{s}^{-1}$ ), quantum yields of photosystems I and II (YI and YII) and non-photochemical fluorescence quenching (NPQ) in pea seedling leaves, calculated using manual (MP) or automatic processing (AP) (scale 10).

**Author Contributions:** Conceptualization, L.K., M.M., and V.V.; methodology, L.K. and M.M.; software, M.M. and L.K.; validation, M.L. and V.S.; formal analysis, M.M., L.K., I.B., and V.S.; investigation, M.M. and M.L.; data curation, M.M., L.K., M.L., and V.S.; writing—original draft preparation, M.M., L.K., and I.B.; writing—review and editing, V.V.; visualization, M.M., M.L., and V.V.; project administration, V.V. All authors have read and agreed to the published version of the manuscript.

**Funding:** This work was supported by the Ministry of Science and Higher Education of the Russian Federation (contract no. 6.3199.2017) for the automatic analysis of electrical signal parameters, and the Russian Science Foundation (project No. 17-76-20032) for the automatic analysis of photosynthetic activity.

**Conflicts of Interest:** The authors declare no conflict of interest.

## References

- Mazars, C.; Thuleau, P.; Lamotte, O.; Bourque, S. Cross-talk between ROS and calcium in regulation of nuclear activities. *Mol. Plant* **2010**, *3*, 706–718. [[CrossRef](#)] [[PubMed](#)]
- Gilroy, S.; Białasek, M.; Suzuki, N.; Górecka, M.; Devireddy, A.R.; Karpiński, S.; Mittler, R. ROS, calcium, and electric signals: Key mediators of rapid systemic signaling in plants. *Plant Physiol.* **2016**, *171*, 1606–1615. [[CrossRef](#)] [[PubMed](#)]
- Sukhov, V.; Sukhova, E.; Vodeneev, V. Long-distance electrical signals as a link between the localaction of stressors and the systemic physiological responses in higher plants. *Prog. Biophys. Mol. Biol.* **2019**, *146*, 63–84. [[CrossRef](#)] [[PubMed](#)]
- Takahashi, F.; Shinozaki, K. Long-distance signaling in plant stress response. *Curr. Opin. Plant Biol.* **2019**, *47*, 106–111. [[CrossRef](#)]
- Gallé, A.; Lautner, S.; Flexas, J.; Fromm, J. Environmental stimuli and physiological responses: The current view on electrical signaling. *Environ. Exp. Bot.* **2015**, *114*, 15–21. [[CrossRef](#)]
- Huber, A.; Bauerle, T. Long-distance plant signaling pathways in response to multiple stressors: The gap in knowledge. *J. Exp. Bot.* **2016**, *67*, 2063–2079. [[CrossRef](#)]
- Szechyńska-Hebda, M.; Lewandowska, M.; Karpiński, S. Electrical signaling, photosynthesis and systemic acquired acclimation. *Front. Physiol.* **2017**, *14*, 684. [[CrossRef](#)]
- Vodeneev, V.; Akinchits, E.; Sukhov, V. Variation potential in higher plants: Mechanisms of generation and propagation. *Plant Signal. Behav.* **2015**, *10*, e1057365. [[CrossRef](#)]
- Hedrich, R.; Salvador-Recatalà, V.; Dreyer, I. Electrical wiring and long-distance plant communication. *Trends Plant Sci.* **2016**, *21*, 376–387. [[CrossRef](#)]
- Rhodes, J.; Thain, J.; Wildon, D. Evidence for physically distinct systemic signalling pathways in the wounded tomato plant. *Ann. Bot.* **1999**, *84*, 109–116. [[CrossRef](#)]
- Vodeneev, V.; Mudrilov, M.; Akinchits, E.; Balalaeva, I.; Sukhov, V. Parameters of electrical signals and photosynthetic responses induced by them in pea seedlings depend on the nature of stimulus. *Funct. Plant Biol.* **2018**, *45*, 160–170. [[CrossRef](#)]
- Sukhov, V. Electrical signals as mechanism of photosynthesis regulation in plants. *Photosynth. Res.* **2016**, *130*, 373–387. [[CrossRef](#)] [[PubMed](#)]

13. Stahlberg, R.; Cleland, R.E.; Van Volkenburgh, E. Slow wave potentials—A propagating electrical signal unique to higher plants. In *Communication in Plants: Neuronal Aspects of Plant Life*; Baluska, F., Mancuso, S., Volkmann, D., Eds.; Springer-Verlag Berlin Heidelberg: Heidelberg, Germany, 2006; pp. 291–308.
14. Katicheva, L.; Sukhov, V.; Akinchits, E.; Vodeneev, V. Ionic nature of burn-induced variation potential in wheat leaves. *Plant Cell Physiol.* **2014**, *55*, 1511–1519. [[CrossRef](#)] [[PubMed](#)]
15. Evans, M.; Morris, R. Chemical agents transported by xylem mass flow propagate variation potentials. *Plant J.* **2017**, *91*, 1029–1037. [[CrossRef](#)]
16. Fromm, J.; Lautner, S. Electrical signals and their physiological significance in plants. *Plant Cell Environ.* **2007**, *30*, 249–257. [[CrossRef](#)]
17. Koziolok, C.H.; Gram, T.H.; Schreiber, U. Transient knockout of photosynthesis mediated by electrical signals. *New Phytol.* **2004**, *161*, 715–722. [[CrossRef](#)]
18. Lautner, S.; Grams, T.E.; Matyssek, R.; Fromm, J. Characteristics of electrical signals in poplar and responses in photosynthesis. *Plant Physiol.* **2005**, *138*, 2200–2209. [[CrossRef](#)]
19. Grams, T.; Lauther, S.; Felle, H.H.; Matyssek, R.; Fromm, J. Heat-induced electrical signals affect cytoplasmic and apoplastic pH as well as photosynthesis during propagation through the maize leaf. *Plant Cell Environ.* **2009**, *32*, 319–326. [[CrossRef](#)]
20. Retivin, V.; Opritov, V.; Lobov, S.; Tarakanov, S.; Khudyakov, V. Changes in the resistance of photosynthesizing cotyledon cells of pumpkin seedlings to cooling and heating, as induced by the stimulation of the root system with KCl solution. *Russ. J. Plant Physiol.* **1999**, *46*, 689–696.
21. Sukhov, V.; Surova, L.; Sherstneva, O.; Vodeneev, V. Influence of variation potential on resistance of the photosynthetic machinery to heating in pea. *Physiol. Plant* **2014**, *152*, 773–783. [[CrossRef](#)]
22. Sukhov, V.; Surova, L.; Sherstneva, O.; Katicheva, L.; Vodeneev, V. Variation potential influence on photosynthetic cyclic electron flow in pea. *Front. Plant Sci.* **2015**, *7*, 766. [[CrossRef](#)] [[PubMed](#)]
23. Sukhov, V.; Surova, L.; Sherstneva, O.; Bushueva, A.; Vodeneev, V. Variation potential induces decreased PSI damage and increased PSII damage under high external temperatures in pea. *Funct. Plant Biol.* **2015**, *42*, 727–736. [[CrossRef](#)]
24. Surova, L.; Sherstneva, O.; Vodeneev, V.; Sukhov, V. Variation potential propagation decreases heat-related damage of pea photosystem I by 2 different pathways. *Plant Signal. Behav.* **2016**, *11*, e1145334. [[CrossRef](#)] [[PubMed](#)]
25. Zandalinas, S.I.; Mittler, R.; Balfagón, D.; Arbona, V.; Gómez-Cadenas, A. Plant adaptations to the combination of drought and high temperatures. *Physiol. Plant* **2018**, *162*, 2–12. [[CrossRef](#)] [[PubMed](#)]
26. Ashraf, M.; Harris, P.J.C. Photosynthesis under stressful environments: An overview. *Photosynthetica* **2013**, *51*, 163–190. [[CrossRef](#)]
27. Zhao, D.J.; Wang, Z.Y.; Huang, L.; Jia, Y.P.; Leng, J.Q. Spatio-temporal mapping of variation potentials in leaves of *Helianthus annuus* L. seedlings in situ using multi-electrode array. *Sci. Rep.* **2014**, *4*, 5435. [[CrossRef](#)] [[PubMed](#)]
28. Astafieva, N. Wavelet-analysis: Basic theory and application examples. *Phys.-Uspekhi* **1996**, *39*, 1085–1108.
29. Addison, P. Wavelet transforms and the ECG: A review. *Phys. Meas.* **2005**, *26*, 155–199. [[CrossRef](#)]
30. Keil, A.; Stolarova, M.; Heim, S.; Gruber, T.; Müller, M.M. Temporary stability of high-frequency brain oscillations in the human EEG. *Brain Topogr.* **2003**, *16*, 101–110. [[CrossRef](#)]
31. Kim, K.H.; Kim, S.J. A Wavelet-based method for action potential detection from extracellular neural signal recording with low signal-to-noise ratio. *IEEE Trans. Biomed. Eng.* **2003**, *50*, 999–1011.
32. Quotb, A.; Bornat, Y.; Renaud, S. Wavelet transform for real-time detection of action potentials in neural signals. *Front. Neuroeng.* **2011**, *4*, 7. [[CrossRef](#)] [[PubMed](#)]
33. Hramov, A.; Koronovskii, A.; Makarov, V.; Pavlov, A.; Sitnikova, E. *Wavelets in Neuroscience*; Springer-Verlag: Berlin/Heidelberg, Germany, 2015; Volume 16, p. 318.
34. Keitt, T.H.; Fischer, J. Detection of scale-specific community dynamics using wavelets. *Ecology* **2006**, *87*, 2895–2904. [[CrossRef](#)]
35. Lió, P. Wavelets in bioinformatics and computational biology: State of art and perspective. *Bioinform. Rev.* **2003**, *19*, 2–9. [[CrossRef](#)] [[PubMed](#)]
36. Haimovich, A.D.; Byrne, B.; Ramaswamy, R.; Welsh, W.J. Wavelet analysis of DNA walks. *J. Comput. Biol.* **2006**, *13*, 1289–1298. [[CrossRef](#)] [[PubMed](#)]

37. Wang, H.F.; Huo, Z.G.; Zhou, G.S.; Liao, Q.H.; Feng, H.K.; Wu, L. Estimating leaf SPAD values of freeze-damaged winter wheat using continuous wavelet analysis. *Plant Physiol. Biochem.* **2016**, *98*, 39–45. [[CrossRef](#)] [[PubMed](#)]
38. Cheng, T.; Rivard, B.; Sánchez-Azofeifa, A.G.; Féret, J.B.; Jacquemoud, S.; Ustin, S.L. Predicting leaf gravimetric water content from foliar reflectance across a range of plant species using continuous wavelet analysis. *J. Plant Physiol.* **2012**, *169*, 1134–1142. [[CrossRef](#)] [[PubMed](#)]
39. Zhang, J.C.; Lin, Y.; Wang, J.H.; Huang, W.J.; Chen, L.P.; Zhang, D.Y. Spectroscopic leaf level detection of powdery mildew for winter wheat using continuous wavelet analysis. *J. Integr. Agric.* **2012**, *11*, 1474–1484. [[CrossRef](#)]
40. Duarte-Galvan, C.; Romero-Troncoso, R.J.; Torres-Pacheco, I.; Guevara-Gonzalez, R.G.; Fernandez-Jaramillo, A.A.; Contreras-Medina, L.M.; Carrillo-Serrano, R.V.; Millan-Almaraz, J.R. FPGA-based smart sensor for drought stress detection in tomato plants using novel physiological variables and discrete wavelet transform. *Sensors (Basel)* **2014**, *14*, 18650–18669. [[CrossRef](#)]
41. Blackburn, G.A.; Ferwerda, J.G. Retrieval of chlorophyll concentration from leaf reflectance spectra using wavelet analysis. *Remote Sens. Environ.* **2008**, *112*, 1614–1632. [[CrossRef](#)]
42. Furon, A.C.; Wagner-Riddle, C.; Ryan Smith, C.; Warland, J.S. Wavelet analysis of wintertime and spring thaw CO<sub>2</sub> and N<sub>2</sub>O fluxes from agricultural fields. *Agric. For. Meteorol.* **2008**, *148*, 1305–1317. [[CrossRef](#)]
43. Von Caemmerer, S.; Farquhar, G.D. Some relationships between the photochemistry and the gas exchange of leaves. *Planta* **1981**, *153*, 376–387. [[CrossRef](#)] [[PubMed](#)]
44. Klughammer, C.; Schreiber, U. Complementary PS II quantum yields calculated from simple fluorescence parameters measured by PAM fluorometry and the saturation pulse method. *PAM Appl. Notes* **2008**, *1*, 27–35.
45. Maxwell, K.; Johnson, G.N. Chlorophyll fluorescence—A practical guide. *J. Exp. Bot.* **2000**, *51*, 659–668. [[CrossRef](#)] [[PubMed](#)]
46. Rioll, O.; Vetterli, M. Wavelets and signal processing. *IEEE Signal Process. Mag.* **1991**, *8*, 14–38. [[CrossRef](#)]
47. Bruce, L.M.; Morgan, C.; Larsen, S. Automated detection of subpixel hyperspectral targets with continuous and discrete wavelet transforms. *IEEE Trans. Geosci. Remote Sens.* **2001**, *39*, 2217–2226. [[CrossRef](#)]
48. Bland, J.M.; Altman, D.G. Measuring agreement in method comparison studies. *Stat. Methods Med. Res.* **1999**, *8*, 135–160. [[CrossRef](#)]
49. Giavarina, D. Understanding bland altman analysis. *Biochem. Med. (Zagreb)* **2015**, *25*, 141–151. [[CrossRef](#)]
50. Grams, T.; Koziolok, C.H.; Lauther, S.; Matyssek, R.; Fromm, J. Distinct roles of electric and hydraulic signals on the reaction of leaf gas exchange upon re-irrigation in *Zea mays* L. *Plant Cell Environ.* **2007**, *30*, 79–84. [[CrossRef](#)]
51. Sukhov, V.; Orlova, L.; Mysyagin, S.; Sinitina, J.; Vodeneev, V. Analysis of the photosynthetic response induced by variation potential in geranium. *Planta* **2012**, *235*, 703–712. [[CrossRef](#)]
52. Sukhova, E.; Mudrilov, M.; Vodeneev, V.; Sukhov, V. Influence of the variation potential on photosynthetic flows of light energy and electrons in pea. *Photosynth. Res.* **2018**, *136*, 215–228. [[CrossRef](#)]
53. Gallé, A.; Lautner, S.; Flexas, J.; Ribas-Carbo, M.; Hanson, D.; Roesgen, J.; Fromm, J. Photosynthetic responses of soybean (*Glycine max* L.) to heat-induced electrical signalling are predominantly governed by modifications of mesophyll conductance for CO<sub>2</sub>. *Plant Cell Environ.* **2013**, *36*, 542–552.
54. Fromm, J.; Hajirezaei, M.R.; Becker, V.K.; Lautner, S. Electrical signaling along the phloem and its physiological responses in the maize leaf. *Front. Plant Sci.* **2013**, *4*, 239. [[CrossRef](#)] [[PubMed](#)]
55. Senhadji, L.; Carrault, G.; Bellanger, J.J.; Passariello, G. Comparing wavelet transforms for recognizing cardiac patterns. *Eng. Med. Biol. Mag.* **1995**, *14*, 167–173. [[CrossRef](#)]
56. Dinh, H.A.N.; Kumar, D.K.; Pah, N.D.; Burton, P. Wavelets for QRS detection. In Proceedings of the 23rd Annual International Conference of the IEEE Engineering in Medicine and Biology Society, Istanbul, Turkey, 25–28 October 2001.
57. Selin, A.; Turunen, J.; Tanttu, J.T. Wavelets in recognition of bird sounds. *EURASIP J. Adv. Signal Process.* **2007**, e051806. [[CrossRef](#)]
58. Lau, K.M.; Weng, H. Climate signal detection using wavelet transform: How to make a time series sing. *Bull. Am. Meteorol. Soc.* **1995**, *76*, 2391–2402. [[CrossRef](#)]
59. Csillag, F.; Kabos, S. Wavelets, boundaries, and the spatial analysis of landscape pattern. *Écoscience* **2002**, *9*, 177–190. [[CrossRef](#)]

60. Bulychev, A.; Komarova, A. Long-distance signal transmission and regulation of photosynthesis in characean cells. *Biochemistry (Moscow)* **2014**, *79*, 273–281. [[CrossRef](#)]
61. Sukhov, V.; Sherstneva, O.; Surova, L.; Katicheva, L.; Vodeneev, V. Proton cellular influx as a probable mechanism of variation potential influence on photosynthesis in pea. *Plant Cell Environ.* **2014**, *37*, 2532–2541. [[CrossRef](#)]
62. Sherstneva, O.; Surova, L.; Vodeneev, V.; Plotnikova, Y.; Bushueva, A.; Sukhov, V. The role of the intra- and extracellular protons in the photosynthetic response induced by the variation potential in pea seedlings. *Biochem. Mosc. Suppl. Ser. A* **2016**, *10*, 60–67. [[CrossRef](#)]
63. Chatterjee, S.K.; Das, S.; Maharatna, K.; Masi, E.; Santopolo, L.; Mancuso, S.; Vitaletti, A. Exploring strategies for classification of external stimuli using statistical features of the plant electrical response. *J. R. Soc. Interface* **2015**, *12*, e20141225. [[CrossRef](#)]
64. Tian, L.; Meng, Q.; Wang, L.; Dong, J.; Wu, H. Research on the effect of electrical signals on growth of sansevieria under Light-Emitting Diode (LED) lighting environment. *PLoS ONE* **2015**, *10*, e0131838. [[CrossRef](#)] [[PubMed](#)]
65. Yang, J.; Du, L.; Gong, W.; Shi, S.; Sun, J.; Chen, B. Potential of vegetation indices combined with laser-induced fluorescence parameters for monitoring leaf nitrogen content in paddy rice. *PLoS ONE* **2018**, *13*, e0191068. [[CrossRef](#)] [[PubMed](#)]
66. Guo, Y.; Zhou, Y.; Tan, J. Wavelet analysis of pulse-amplitude-modulated chlorophyll fluorescence for differentiation of plant samples. *J. Theor. Biol.* **2015**, *370*, 116–120. [[CrossRef](#)] [[PubMed](#)]
67. Pereira, D.R.; Papa, G.P.; Saraiva, G.F.R.; Souza, G.M. Automatic classification of plant electrophysiological responses to environmental stimuli using machine learning and interval arithmetic. *Comput. Electron. Agric.* **2018**, *145*, 35–42. [[CrossRef](#)]
68. Chen, Y.; Zhao, D.J.; Wang, Z.Y.; Wang, Z.Y.; Tang, G.; Huang, L. Plant electrical signal classification based on Waveform. *Algorithms* **2016**, *9*, 70. [[CrossRef](#)]
69. Chatterjee, S.K.; Malik, O.; Gupta, S. Chemical sensing employing plant electrical signal response-classification of stimuli using curve fitting coefficients as features. *Biosensors (Basel)* **2018**, *8*, 83. [[CrossRef](#)]
70. Gamon, J.A.; Peñuelas, J.; Field, C.B. A narrow-waveband spectral index that tracks diurnal changes in photosynthetic efficiency. *Remote Sens. Environ.* **1992**, *41*, 35–44. [[CrossRef](#)]
71. Peñuelas, J.; Filella, I.; Gamon, J.A. Assessment of photosynthetic radiation-use efficiency with spectral reflectance. *New Phytol.* **1995**, *131*, 291–296. [[CrossRef](#)]
72. Sukhova, E.; Sukhov, V. Analysis of light-induced changes in the photochemical reflectance index (PRI) in leaves of pea, wheat, and pumpkin using pulses of green-yellow measuring light. *Remote Sens.* **2019**, *11*, 810. [[CrossRef](#)]
73. Sukhov, V.; Sukhova, E.; Gromova, E.; Surova, L.; Nerush, V.; Vodeneev, V. The electrical signals-induced systemic photosynthetic response is accompanied with changes in photochemical reflectance index in pea. *Funct. Plant Biol.* **2019**, *46*, 328–338. [[CrossRef](#)]
74. Garbulsky, M.F.; Peñuelas, J.; Gamon, J.; Inoue, Y.; Filella, I. The photochemical reflectance index (PRI) and the remote sensing of leaf, canopy and ecosystem radiation use efficiencies. A review and meta-analysis. *Remote Sens. Environ.* **2011**, *115*, 281–297. [[CrossRef](#)]
75. Zhang, C.; Filella, I.; Garbulsky, M.F.; Peñuelas, J. Affecting factors and recent improvements of the photochemical reflectance index (PRI) for remotely sensing foliar, canopy and ecosystemic radiation-use efficiencies. *Remote Sens.* **2016**, *8*, 677. [[CrossRef](#)]
76. Sukhova, E.; Sukhov, V. Connection of the photochemical reflectance index (PRI) with the photosystem II quantum yield and nonphotochemical quenching can be dependent on variations of photosynthetic parameters among investigated plants: A meta-analysis. *Remote Sens.* **2018**, *10*, 771. [[CrossRef](#)]

